A Modified T-ESPRIT for 2-D Direction of Arrival Estimation Performance Enhancement

Youssef Fayad and Qunsheng Cao

***Abstract*—A new algorithm for improving 2D-Direction of Arrival Estimation (2D-DOAE) accuracy and estimator performance has been carried out. Subspace concept has been employed into ESPRIT method to reduce the computational complexity and the model's non-linearity effect into 2D-DOAE problem. The algorithm accuracy is verified by closed-form Cramér–Rao bound (CRB). The simulation results show that the proposed algorithm realizes estimation process better than those of the previous estimation techniques leading to the estimator performance enhancement.**

***Index Terms*—DOAE, Subspace, ESPRIT, angle glint.**

I. Introduction

Estimating of direction-of-arrival is a very important process in many signal processing applications. DOAE is the creator of the tracking gate dimensions (the azimuth and the elevation). Accurate DOAE leads to reduce the angle glint error which affects the accuracy of the tracking radars. ESPRIT has been widely studied in one-dimensional (1D) DOAE for uniform linear array (ULA), non-uniform linear array (NULA) [1]-[11], and also extended to two-dimensional (2D) DOAE [12]-[19]. A high performance for the estimator means high accuracy of DOAE with low calculation costs.

In this paper, a new modified algorithm based on time multi resolution (T-ESPRIT) [1], [2] is presented to estimate 2D-DOAE (azimuth and elevation) of a radiated source which has been detected by a planar array antenna. Subspace concept has been applied to reduce the model's non-linearity effect and to realize parallel processing which leads to enhance the estimation accuracy with low computational load.

The reminder of the paper is organized as follows. In Section II, the two dimensions time multi resolution ESPRIT (2D T-ESPRIT) DOAE technique has been introduced, the Cramér–Rao bounds (CRB) is presented in Section III, in Section IV the simulation results are presented, and Section V is conclusions.

II. Proposed Algorithm

A. The Measurement Model

In this model, the radiation propagates in straight lines due to isotropic and non-dispersive transmission medium assumption. Also, it is assumed that the sources as a far-field away the array. Consequently, the radiation impinging on the array is a summation of the plane waves. The signals are assumed to be narrow-band processes, and they can be considered to be sample functions of a stationary stochastic process or deterministic functions of time. Considering there are K narrow-band signals, and the center frequency f is assumed to have same $\omega_0 = 2\pi f$, for the k^{th} signal can be written as:

$$s_k(t) = E_k e^{j(\omega_0 t + \Psi_k)}, k = 1, 2, \dots, K \quad (1)$$

where, $s_k(t)$ is the signal of the k^{th} emitting source at time instant t, Ψ_k is the carrier phase angles are assumed to be random variables, each uniformly distributed on $[0,2\pi]$ and all statistically independent of each other, and E_k is the incident electric field, can be written as components form. As a general expression, we omit the subscript, then

$$\vec{E} = E_\theta \hat{e}_\theta + E_\varphi \hat{e}_\varphi \quad (2)$$

where E_φ and E_θ are the horizontal and the vertical components of the field, respectively.
Defining $\gamma \in [0, \pi/2]$ as the auxiliary polarization angle, $\eta \in [-\pi, \pi]$ as the polarization phase difference, then,

$$E_\varphi = |\vec{E}| \cos\gamma, E_\theta = |\vec{E}| \sin\gamma e^{j\eta}. \quad (3)$$

The incident field can be also expressed in Cartesian coordinate system,

$$\vec{E} = E_\theta \hat{e}_\theta + E_\varphi \hat{e}_\varphi = (E_\theta \cos\theta \cos\varphi - E_\varphi \sin\varphi)\hat{e}_x + (E_\theta \cos\theta \sin\varphi + E_\varphi \cos\varphi)\hat{e}_y + (E_\theta \sin\theta)\hat{e}_z \quad (4)$$

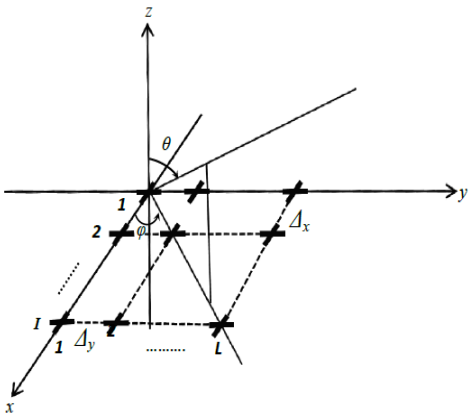

Fig. 1. Planar antenna array.

Fig. 1 shows a planar antenna array has elements indexed L, I along y and x directions, respectively. For any pairs (i, l), its coordinate is $(x, y) = ((i\text{-}1)\,\Delta_x, (l\text{-}1)\,\Delta_y)$, where $i=1,\dots,I$, $l=1,\dots,L$, Δ_x and Δ_y are reference displacements between neighbor elements along x and y axis. The array elements are oriented in xoy plane, the space phase factors along x

Manuscript received April 30, 2015; revised June 20, 2015.

The authors are with College of Electronic and Information Engineering, Nanjing University of Aeronautics& Astronautics, Nanjing 210016, China (e-mail: youseffyad@nuaa.edu.cn, qunsheng@nuaa.edu.cn).

and *y* directions are expressed as.

$$p_i(\theta_k,\varphi_k) \equiv p_i^k = e^{j\frac{2\pi(i-1)\Delta_x}{\lambda}\sin\theta_k\cos\varphi_k} \quad (5a)$$

$$q_l(\theta_k,\varphi_k) \equiv q_l^k = e^{j\frac{2\pi(l-1)\Delta_y}{\lambda}\sin\theta_k\sin\varphi_k} \quad (5b)$$

where, (θ_k,φ_k) denote the k^{th} source elevation angle and azimuth angle respectively, and λ is the wavelength of the k^{th} signal. The measurement vector can be expressed as,

$$z_{i,l}(t) = \sum_{k=1}^{K} u_k s_k(t) p_i(\theta_k,\varphi_k) q_l(\theta_k,\varphi_k) + w_{i,l}(t) \quad (6a)$$

$$[Z(t)] = \left[z_{1,1}(t) \cdots z_{1,L}(t) \cdots z_{I,1}(t) \cdots z_{I,L}(t)\right]^T \quad (6b)$$

where $[W(t)]$ stands for the additive white Gaussian noise (AWGN), it is consisted as,

$$[W(t)] = \left[w_{1,1}(t) \cdots w_{1,L}(t) \cdots w_{I,1}(t) \cdots w_{I,L}(t)\right]^T \quad (7)$$

From Eqs. (3) and (4), we got

$$u_k = \begin{pmatrix} \sin\gamma_k\cos\theta_k\cos\varphi_k\, e^{j\eta_k} - \cos\gamma_k\sin\varphi_k \\ \sin\gamma_k\cos\theta_k\sin\varphi_k e^{j\eta_k} + \cos\gamma_k\cos\varphi_k \end{pmatrix} \quad (8)$$

For receiving array, the whole receiving factors in subspaces matrix are included in $[a(\theta_k,\varphi_k)]$ that is,

$$a(\theta_k,\varphi_k) \triangleq^{\text{def}} p(\theta_k,\varphi_k) \otimes q(\theta_k,\varphi_k) \quad (9)$$

where $\otimes$ denotes the Kronker product, so

$$A(\theta_k,\varphi_k) = [u_k^T p_1^k q_1^k\ u_k^T p_1^k q_2^k \ldots u_k^T p_1^k q_L^k\ \ u_k^T p_2^k q_1^k\ \ u_k^T p_2^k q_2^k \cdots u_k^T p_2^k q_L^k \cdots u_k^T p_I^k q_1^k\ u_k^T p_I^k q_2^k \cdots u_k^T p_I^k q_L^k]^T \quad (10)$$

The receiving model can be rewritten as,

$$[Z(t)] = [A]S(t) + [W(t)] \quad (11)$$

where $S(t) \triangleq^{\text{def}} [s_1(t) \cdots \cdots s_K(t)]^T$ and, $[A] \triangleq^{\text{def}} \left[A(\theta_1\varphi_1) \cdots \cdots A(\theta_K,\varphi_K)\right]$

The subspace approach not only decreases the computational load as a result of shrinking the matrix dimensions, but it also reduces the influence of non-linearity when deals with signal inside each small time step as a linear part.

For the electronic scanning beam (ESB) with width W_{az} scans β sector, the hit time T_D is obtained as follow [20],

$$T_D = \frac{W_{az}\times 60}{\beta\times\vartheta} \quad (12)$$

where ϑ is the number of scans per minute,

$$Number\ of\ hits = T_D \times PRF \quad (13)$$

where *PRF* is the pulse recurrence frequency.

Using the T-ESPRIT method, the whole data is divided into M snapshots at each time $T = T_D/M$ second. Then it picks up enough data r enclosed by each snapshot m with time period $\tau = \frac{T}{r}$ as short as possible. So, from Eq. (11) each receiving signal measurement value through m^{th} subspace is given as,

$$[z^m(\tau)] = [A]s^m(\tau) + [w^m(\tau)] \quad (14)$$

The index m runs as m =1, 2, …, M snapshots. Therefore, the whole data matrix can be expressed as,

$$\mathbf{Z} \triangleq^{\text{def}} \begin{bmatrix} z_{1,1}^1(0) & \ldots & z_{1,1}^1(\tau_1)\ldots\ldots z_{1,1}^m(0) & \ldots & z_{1,1}^m(\tau_1)\ldots\ldots z_{1,1}^M(0) & \ldots & z_{1,1}^M(\tau_1) \\ \vdots & \ddots & \vdots \quad \vdots & \ddots & \vdots \quad \vdots & \ddots & \vdots \\ z_{I,L}^1(0) & \ldots & z_{I,L}^1(\tau_1)\ldots\ldots z_{I,L}^m(0) & \ldots & z_{I,L}^m(\tau_1)\ldots\ldots z_{I,L}^M(0) & \ldots & z_{I,L}^M(\tau_1) \end{bmatrix} \quad (15)$$

where, $\tau_1 = (r-1)\times\tau$.

The dimension of [Z] for the k^{th} signal is $2(I{\cdot}L{\cdot}Mr)$. For the m^{th} subspace data matrix can be expressed as,

$$[z^m(\tau)] = \begin{bmatrix} z_{1,1}^m(0) & \ldots & z_{1,1}^m(\tau_1) \\ \vdots & \ddots & \vdots \\ z_{I,L}^m(0) & \ldots & z_{I,L}^m(\tau_1) \end{bmatrix} \quad (16)$$

For T-ESPRIT scheme the ESPRIT algorithm is used in an appropriate picked data represented in (15) for each (m) subspace - shown in (16) - in parallel for the same sampling accuracy thus reducing the calculations load and consequently saving time is achieved. Fig. 2 is given the diagram of a 2D T-ESPRIT method, Fig. 3 is the time baseline and the time series which indicates the subspace approach.

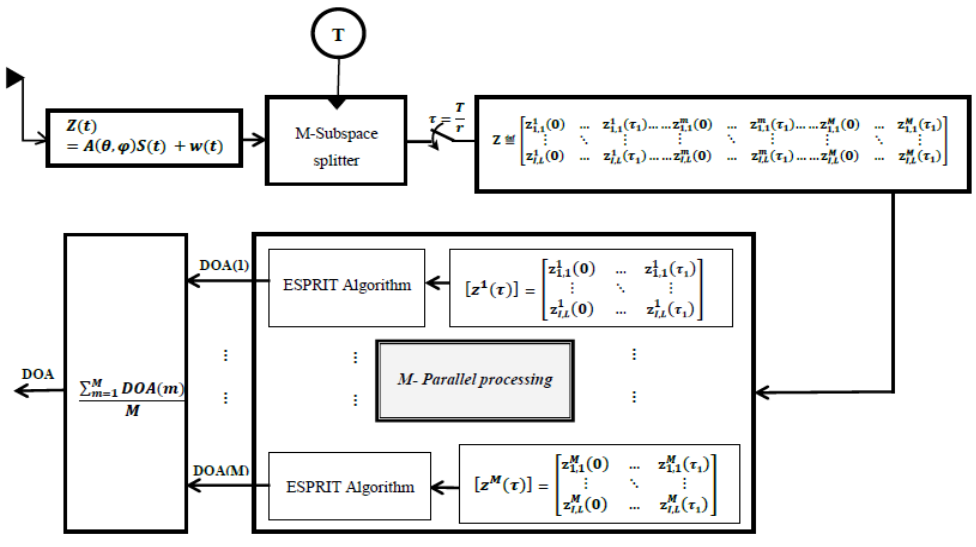

Fig. 2. Planar array T-ESPRIT technique.

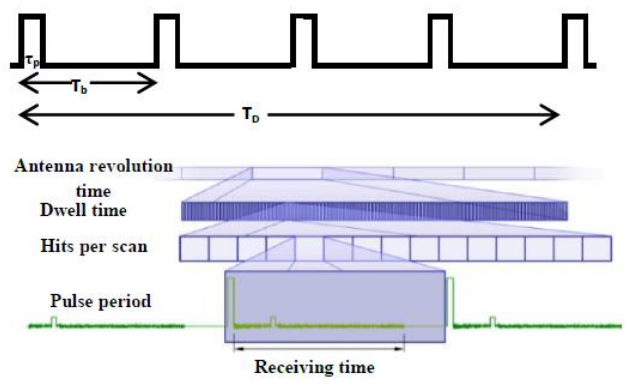

(a).

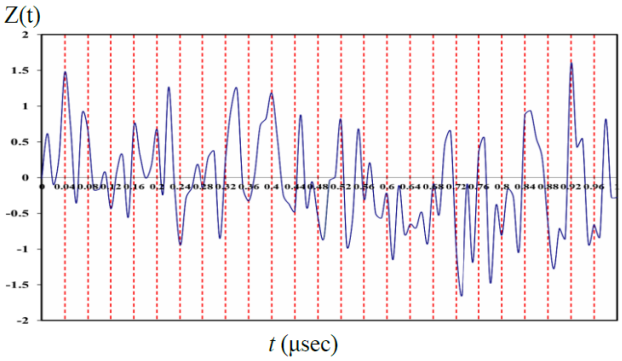

(b).

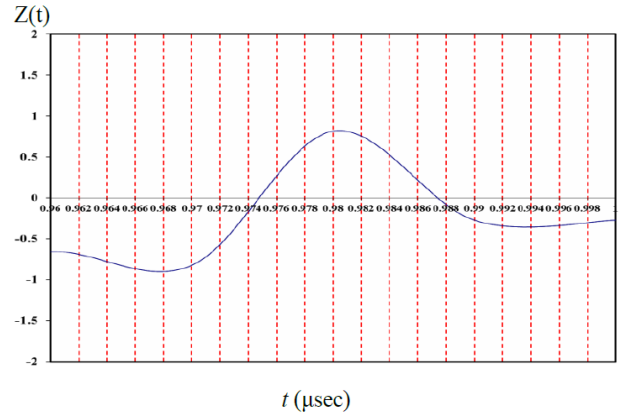

(c).

Fig. 3. (a). Time- baseline, (b). Total signal in time series, (c). signal in 25th snapshot.

B. T-Esprit Method for 2-D Doae

The ESPRIT algorithm is based on a covariance formulation that is,

$$\hat{R}_{zz} \stackrel{\text{def}}{=} E[Z(\tau)Z(\tau)^H] = A\hat{R}_{ss}A^H + \sigma^2\Sigma_w \quad (17)$$

$$\hat{R}_{ss} = E[S(\tau)S^H(\tau)] \quad (18)$$

where $\hat{R}_{zz}$ is the correlation matrix of the array output signal matrix, $\hat{R}_{ss}$is the autocorrelation matrix of the signal. The subscript H denotes the complex conjugate transpose.

The correlation matrix of $\hat{R}_{zz}$ can be done for eigenvalue decomposition as follow,

$$\hat{R}_{zz} \stackrel{\text{def}}{=} \hat{E}_S\Lambda\hat{E}_S^H + \sigma^2\hat{E}_N\Lambda\hat{E}_N^H \quad (19)$$

where the eigenvalues are ordered $\lambda_1 > \lambda_2 > \cdots > \lambda_K > \lambda_{K+1} > \lambda_{K+1} = \cdots = \lambda_{2(I\times L)} = \sigma^2$. The eigenvectors $\hat{E}_S = [\hat{e}_1, \hat{e}_2, \cdots, \hat{e}_K]$ for larger K eigenvalues spans the signal subspace, the rest $2(I\times L) - K$ smaller eigenvalues $\hat{E}_N = [\hat{e}_{K+1}, \cdots, \hat{e}_{2(I\times L)}]$ spans the noise subspace which is orthogonal to the signal subspace. Therefore, there exists a unique nonsingular matrix Q, such that

$$\hat{E}_S = [A]Q = [u_k^T \otimes p_i(\theta_k, \varphi_k) \otimes q_l(\theta_k, \varphi_k)]Q \quad (20)$$

In Eq. (10) let A_{P1} and A_{P2} be the first and the last $2L\times(I-1)$ rows of A respectively, they differ by the factor $\Delta p_k = e^{j\frac{2\pi\Delta_x}{\lambda}\sin\theta_k\cos\varphi_k}$ along the x direction. So $A_{P2} = A_{P1}\emptyset_P$, where $\emptyset_P$ is the diagonal matrix with diagonal elements Δp_k. Consequently, $\hat{E}_{P1}$ and $\hat{E}_{P2}$ will be the first and the last $2L\times(I-1)$ sub-matrices formed from $\hat{E}_S$. Then the diagonal elements p_k of $\emptyset_P$ are the eigenvalues of the unique matrix $\Psi_P = Q^{-1}\emptyset_P Q$, that satisfies

$$\hat{E}_{P2} = \hat{E}_{P1}\Psi_P. \quad (21a)$$

Similarly, the two $2I\times(L-1)$ sub-matrices A_{q1} and A_{q2} consist of the rows of A numbered $2L\times(i-1)+l$ and $2L\times(i-1)+l+2$ respectively, differ by the space factors $\Delta q_k = e^{j\frac{2\pi\Delta_y}{\lambda}\sin\theta_k\sin\varphi_k}$ along the y direction, $l=1,\ldots,2(L-1)$. Then $A_{q2} = A_{q1}\emptyset_q$ where $\emptyset_q$ is the diagonal matrix with diagonal elements Δq_k. Consequently, $\hat{E}_S$ forms the $2I\times(L-1)$ two sub-matrices $\hat{E}_{q1}$ and $\hat{E}_{q2}$. Then the diagonal elements Δq_k of $\emptyset_q$, are the eigenvalues of the unique matrix $\Psi_q = Q^{-1}\emptyset_q Q$, that satisfies,

$$\hat{E}_{q2} = \hat{E}_{q1}\Psi_q \quad (21b)$$

Therefore, the arrival angles (θ_k, φ_k)can be calculated as:

$$\theta_k = \sin^{-1}\left\{\frac{\lambda}{2\pi}\left[\left(\frac{arg(\Delta p_k)}{\Delta_x}\right)^2 + \left(\frac{arg(\Delta q_k)}{\Delta_y}\right)^2\right]^{1/2}\right\} \quad (22)$$

$$\varphi_k = \tan^{-1}\left[\frac{\Delta_x}{\Delta_y}\cdot\frac{arg(q_k)}{arg(p_k)}\right] \quad (23)$$

III. Cramér–Rao Bounds (CRB) for the 2D Case

The Cramér–Rao bound has provided more accuracy achievable by any unbiased estimator of signal parameters and fundamental physical limit on system accuracy [21]-[22]. For Gaussian process, M snapshots, and response $A(\theta,\varphi)$ corresponding sensors $I\times L$, it has

$$P(Z/(\theta,\varphi)) = \frac{1}{\sqrt{2\pi\delta^2}}e^{\frac{\sum_{m=1}^{M}-(Z_m-S_mA(\theta,\varphi))(Z_m-S_mA(\theta,\varphi))^T}{2\delta^2}} \quad (24)$$

Substitute with

$$F_m = Z_m - S_mA(\theta,\varphi) \quad (25)$$

Then we have,

$$ln\,P(Z|(\theta,\varphi)) = ln\frac{1}{\sqrt{2\pi\delta^2}} - \frac{1}{2\delta^2}\sum_{m=1}^{M}(F_m)(F_m)^T \quad (26)$$

To get the CRB we first calculate$E\left[\frac{\partial^2 ln\,P(Z/(\theta,\varphi))}{\partial\theta\,\partial\varphi}\right]$, which denotes the expected value (sample mean)

$$E\left[\frac{\partial^2 \ln P(Z/(\theta,\varphi))}{\partial\theta\,\partial\varphi}\right] = -\frac{M}{\sigma^2}\cdot E\left[\begin{pmatrix} \frac{\partial^2 J}{\partial\theta^2} & \frac{\partial^2 J}{\partial\theta\partial\varphi} \\ \frac{\partial^2 J}{\partial\varphi\partial\theta} & \frac{\partial^2 J}{\partial\varphi^2}\end{pmatrix}\right] \quad (27)$$

where $J = \frac{1}{2}F_m F_m^T$.

For simplicity let F_m denoted by F,

$$\frac{\partial J}{\partial\theta} = \frac{\partial J}{\partial F}\frac{\partial F}{\partial\theta} + \frac{\partial J}{\partial F^T}\frac{\partial F^T}{\partial\theta}, \frac{\partial J}{\partial\varphi} = \frac{\partial J}{\partial F}\frac{\partial F}{\partial\varphi} + \frac{\partial J}{\partial F^T}\frac{\partial F^T}{\partial\varphi} \quad (28)$$

$$FIM = -E\left[\frac{\partial^2 \ln P(Z|(\theta,\varphi))}{\partial\theta\,\partial\varphi}\right] \quad (29)$$

where *FIM* expresses the Fisher Information Matrix. Substitute from Eq. (25) into Eq, (28) then into Eqs. (27) and (29), we got,

$$FIM = 2M\left(\frac{S}{\delta}\right)^2 Real\begin{bmatrix} \frac{\partial\left(A^T(\theta,\varphi)\right)}{\partial\theta}\frac{\partial(A(\theta,\varphi))}{\partial\theta} & \frac{\partial\left(A^T(\theta,\varphi)\right)}{\partial\varphi}\frac{\partial(A(\theta,\varphi))}{\partial\theta} \\ \frac{\partial\left(A^T(\theta,\varphi)\right)}{\partial\theta}\frac{\partial(A(\theta,\varphi))}{\partial\varphi} & \frac{\partial\left(A^T(\theta,\varphi)\right)}{\partial\varphi}\frac{\partial(A(\theta,\varphi))}{\partial\varphi}\end{bmatrix} \quad (30)$$

Finally, we have,

$$CRB = [FIM]^{-1} \quad (31)$$

IV. Simulation Results and Comparisons

Considering the 2D-DOAE process with the AWGN, the parameters are given T_D=1msec, $\beta = 90°$, W_{az} = 1.5°, number of hits = 4, $\vartheta = 1000$ scan/min, and f_s = 25 MHz. Assuming total 25 temporal snapshots, pickup enclosed data r =20 times, 200 independent Monte Carlo simulations, and SNR = -5 to15dB. In order to validate the T-ESPRIT method, it has used in the planar case with different number of elements, such as (I, L) = (5, 5) and (6, 6) with displacement values $\Delta_x = \Delta_y = \lambda/2$, with θ=45° and φ=60°. Fig. 4 (a) and Fig. (b) are depicted the subspace DOAE process. It is found that the computational load was reduced as a result of reducing the measurement matrix dimension to ($2IL \times r$) instead of ($2IL \times Mr$) and employ the subspaces parallel processing concept. Table I represents the computational time and complexity of the proposed method in term of number of flip-flops. It is obvious that the computational load has been reduced as a result of applying the ESPRIT algorithm on the captured r data for each m subspace $[z^m(\tau)]_{(2IL\times r)}$ in parallel, it gives us a simultaneous processing for M subspaces with each has r snapshots instead of processing for one space has a large number of snapshots d, (d=Mr) snapshots.

TABLE I: Comparison of the Required Computation Time and Complexity

Computational	Conventional ESPRIT	Proposed algorithm
time (msec)	16.78	1.62
complexity	$O(4d(IL)^2+8(IL)^3)$	$O(M+4r(IL)^2+8(IL)^3)$

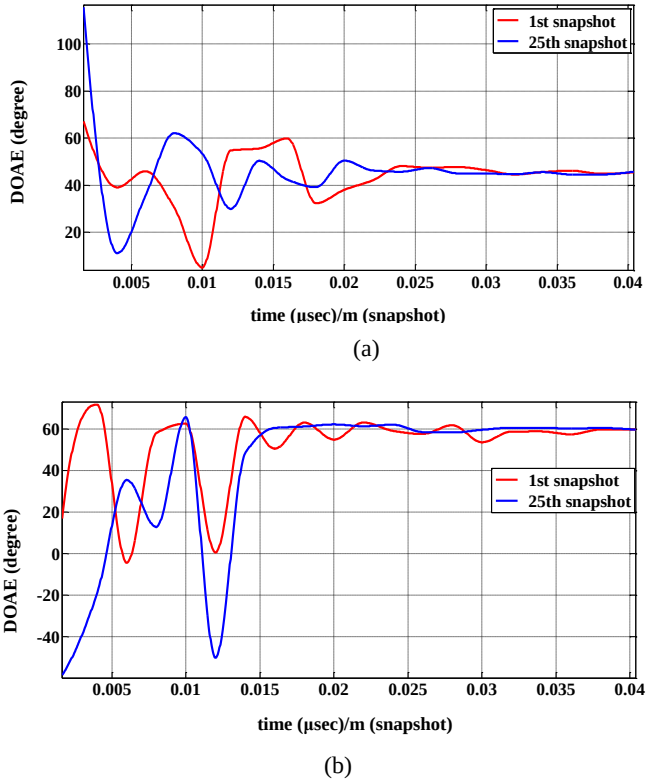

Fig. 4. Implementation of the T-ESPRIT method for the PA for $\Delta_x = \Delta_y = \lambda/2$, (a) θ=45°, (b) φ=60°.

Fig. 5 presents the T-ESPRIT RMSEs for different number of elements. The T-ESPRIT errors are close to the CRB.

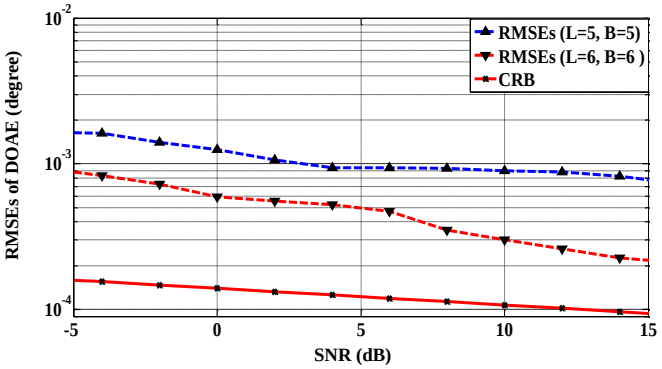

Fig. 5. The RMSEs of T-ESPRIT method for PA with different number of elements for $\Delta_x = \Delta_y = \lambda/2$, at θ=45°, φ=60°.

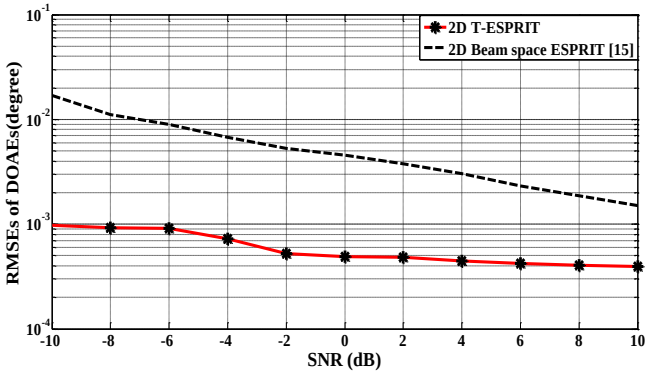

Fig. 6. RMSEs vs. SNR for T-ESPRIT with the doppler effect embedding and beam space-ESPRIT methods.

The accuracy improvement of the 2D-DOAE using proposed algorithm (T-ESPRIT) has been verified by comparing the resulted RMSEs with the RMSEs of 2D-Beamspace ESPRIT (DFT-ESPRIT) algorithm used in Ref. [15]. Fig. 6 shows comparison between the proposed algorithm errors and errors of the algorithm used in Ref. [15].

A comparison results displayed in Fig. 6 show that the errors of the proposed algorithm are less than the errors of 2D- DFT Beamspace ESPRIT algorithm [15]. This upgrade has been realized due to the increase of DOAE accuracy when using the T-ESPRIT algorithm applying the subspace approach which decreases the errors caused by the model nonlinearity effect. Results in table.I indicates that the proposed algorithm requires $O(M+4r(IL)^2+8(IL)^3)$ flops, while the conventional ESPRIT algorithm needs $O(4d(IL)^2+8(IL)^3)$ flops. Also it notes from this table that the developed ESPRIT algorithm requires only about 9.7% of the computational time that required in the classical ESPRIT algorithm.

Simply, we can say that the developed ESPRIT method achieved success into increasing the DOAE accuracy with low computational load leading to increase the estimator efficacy.

V. Conclusions

In this paper, we have developed a new T-ESPRIT method based on the concept of subspace processing and time series to solve the 2D-DOAE, which divided the data into subspaces, then applied ESPRIT on the picked up data enclosed by each subspace in parallel leading to reduce the non-linearity effect and decrease the calculations time. It has been found that the estimation accuracy has been increased with low computational load. Also the computational time is reduced by 90%. The proposed algorithm realized the estimator performance enhancement.

References

[1] Y. Fayad, C. Wang, Q. S. Cao, and A. E. D. S. Hafez, "A developed ESPRIT algorithm for DOA estimation," *Frequenz*, vol. 69, no. 3, pp. 263–269, 2015.

[2] Y. Fayad, C. Wang, Q. S. Cao, and A. E. D. S. Hafez, "Direction of arrival estimation using novel ESPRIT method for localization and tracking radar systems," in *Proc. the IEEE 11th International Bhurban Conference on Applied Sciences & Technology (IBCAST)*, Islamabad, Pakistan, January 14–18, 2014, pp. 396-398.

[3] N. Nordkvist and A. K. Sanyal, "Attitude feedback tracking with optimal attitude state estimation," in *Proc. the Conference on American Control*, 2010, pp. 2861-2866.

[4] R. Roy, A. Paulraj, and T. Kailath, "ESPRIT-estimation of signal parameters via rotational invariance techniques, acoustic, speech, and signal processing," in *Proc. the IEEE International Conference on ICASSP*, 1986, vol. 11. pp. 2495-2498.

[5] R. H. Roy, "ESPRIT-Estimation of signal parameters via rotational invariance techniques," Ph.D. dissertation, Stanford Univ. Stanford, CA, 1987.

[6] R. Roy and T. Kailath, "ESPRIT-estimation of signal parameters via rotational invariance techniques," *IEEE Transaction on Acoustic, Speech, and Signal Processing*, vol. 37, no. 7, pp. 984-995, 1989.

[7] Z. I. Khan, R. A. Awang, A. A. Sulaiman, M. H. Jusoh, N. H. Baba, M. MD. Kamal, and N. I. Khan, "Performance analysis for estimation of signal parameters via rotational invariance technique (ESPRIT) in estimating direction of arrival for linear array antenna," in *Proc. the Conference on IEEE International RF And Microwave*, Kuala Lumpur, Malaysia, December 2-4, 2008.

[8] A. N. Lemma, A. J. V. D. Veen, and E. F. Deprettere, "Joint angle-frequency estimation using multi-resolution esprit," in *Proc. the IEEE International Conference on Acoustics, Speech and Signal Processing*, 1998, vol. 4, pp. 1957-1960.

[9] G. M. Xu and J. G. Huang "Multi-resolution parameters estimation for polarization sensitivity array," in *Proc. the IEEE International Symposium on Knowledge Acquisition and Modeling Workshop, KAM*, 2008, pp. 180-183.

[10] V. Vasylyshyn, "Direction of arrival estimation using esprit with sparse arrays," in *Proc. the Conference on EUMA-6th European Radar*, 2009.

[11] A. N. Lemma, A. J. V. D. Veen, and E. F. Deprettere, "Multiresolution esprit algorithm," *IEEE Transaction on Signal Processing*, vol. 47, no. 6, pp. 1722-1726, 1999.

[12] F. Gao and A. B. Gershman, "A generalized ESPRIT approach to direction of arrival estimation," *IEEE Signal Processing Letters*, vol. 12, no. 3, pp. 254–257, 2005.

[13] A. L Swindlehurst, B. Ottersten, R. Roy, and T. Kailath, "Multiple invariance ESPRIT," *IEEE Transactions on Signal Processing*, vol. 40, no. 4, pp. 867–881, 1992.

[14] J. Li and R. T. Compton, "Two-dimensional angle and polarization estimation using the esprit algorithm," *IEEE Transactions on Antennas and Propagation*, vol. 40, no. 5, pp. 550-555, 1992.

[15] C. P. Mathews, M. Haardt, and M. D. Zoltowski, "Performance analysis of closed-form, esprit based 2-D angle estimator for rectangular arrays," *IEEE Signal Processing Letters*, vol. 3, no. 4, pp. 124-126, 1996.

[16] Y. Zhang, Z. Ye, X. Xu, and J. Cui, "Estimation of two-dimensional direction-of-arrival for uncorrelated and coherent signals with low complexity," *IET Radar Sonar Navigation*, vol. 4, no. 4, pp.507-519, 2010.

[17] F. J. Chen, S. Kwong, and C. W. Kok, "Esprit-like two-Dimensional DOA estimation for coherent signals," *IEEE Transactions on Aerospace and Electronic Systems*, vol. 46, no. 3, pp. 1477-1484, 2010.

[18] J. Hui and Y. Gang, "An improved algorithm of ESPRIT for signal DOA estimation," in *Proc. the International Conference on Industrial Control and Electronics Engineering*, pp. 317-320.

[19] X. Xu and Z. Ye, "Two-dimensional direction of arrival estimation by exploiting the symmetric configuration of uniform rectangular array," *IET Radar Sonar Navigation*, vol. 6, no. 5, pp. 307-313, 2012.

[20] C Wolff, Radar Basics. (2015). [Online]. Available: http://www.radartutorial.eu

[21] A. N. D. Andrea, U. Mengali, and R. Reggiannini, "The modified Cramer-rao bound and its application to synchronization problems," *IEEE Transaction on Communication*, vol. 42, no. 2, pp. 1391-1399, 1994.

[22] S. T. Smith, "Statistical resolution limits and the Complexified Cramér–Rao bound," *IEEE Transaction on Signal Processing*, vol. 53, no. 5, pp. 1597-1609, May, 2005.

Youssef Fayad was born in Alexandria Egypt, in 1975. He received the B.S. in electronic engineering and the M.S. in communications and electronics from Faculty of Engineering, Alexandria University, Egypt, in 1997, 2010 respectively. He is currently pursuing his Ph.D. degree in radar system in Nanjing University of Aeronautics and Astronautics, College of Electronic and Information Engineering, Nanjing, china. He is a student member of IEEE, he is also working as an assistant lecturer in Air Defense College, Egypt. His research interests are antenna and radar signal processing.

Qunsheng Cao received his Ph.D. in electrical engineering from the Hong Kong Polytechnic University in 2001. From 2001 to 2005 he worked as a research associate in the Department of Electrical Engineering, University of Illinois at Urbana-Champaign and at the Army High Performance Computing Research Center (AHPCRC), University of Minnesota. In 2006, Dr. Cao joined the Nanjing University of Aeronautics and Astronautics (NUAA), China, as a professor of electrical engineering. Dr. Cao's current research interests are in computational electromagnetics, antenna and microwave technology and the radar signal processing. Dr. Cao has published more than 120 academic papers in refereed journals and conference proceedings.